



On a hyperfine interaction in ϵ -Fe

Dimitrios Bessas¹  · Ilya Sergueev² · Konstantin Glazyrin² · Cornelius Strohm² · Ilya Kuppenko^{1,3} · Daniel G. Merkel^{1,4} · Aleksandr I. Chumakov¹ · Rudolf Ruffer¹

Published online: 2 December 2019
© Springer Nature Switzerland AG 2019

Abstract

We explore alternative ways to Mössbauer spectroscopy such as nuclear forward scattering of synchrotron radiation, and synchrotron radiation perturbed angular correlation spectroscopy to reveal the elusive and long-sought hyperfine interactions in ϵ -Fe. We indicate that synchrotron radiation perturbed angular correlation spectroscopy is the most viable method.

Keywords ϵ -Fe · Hexaferrum · High pressure · Hyperfine interactions · Mössbauer spectroscopy · Nuclear forward scattering · Synchrotron radiation perturbed angular correlation

1 Introduction

According to present knowledge on the phase diagram of iron, a transition from the familiar ferromagnetic α -phase (body centered cubic; ambient pressure and temperature) to a high pressure non-magnetic ϵ -phase hexagonal closed packed, known as hexaferrum, takes place in a wide pressure and temperature range. The hyperfine interactions in ϵ -Fe have been studied using Mössbauer spectroscopy, however, this topic is highly debated.

Mössbauer spectroscopy utilizing a conventional radioactive source is not the most suitable technique when the potential hyperfine interactions lead to an energy splitting in the nuclear levels, i.e., less or equal to $\Gamma_0 = 4.6$ neV, i.e., the energy width of the first nuclear excited state in the cascade of ^{57}Fe .

This article is part of the Topical Collection on *Proceedings of the International Conference on the Applications of the Mössbauer Effect (ICAME2019), 1-6 September 2019, Dalian, China*
Edited by Tao Zhang, Junhu Wang and Xiaodong Wang

✉ Dimitrios Bessas
bessas@esrf.fr

¹ ESRF - The European Synchrotron, F-38043, Grenoble, France

² Deutsches Elektronen-Synchrotron, 22607 Hamburg, Germany

³ Present address: Institut für Mineralogie, Universität Münster, 48149 Münster, Germany

⁴ Institute for Particle and Nuclear Physics, Wigner Research Centre for Physics, Hungarian Academy of Sciences, H-1525 Budapest, Hungary

Conventional Mössbauer spectroscopy is, moreover, not a well suited technique for characterizing samples under high pressure. This is because in samples with dimensions particularly smaller than $100\ \mu\text{m}$ a point-like radioactive source at a very short distance from the sample must be used in order to efficiently utilize the radiation provided by the source. However, the energy spread of the radiation emitted by a radioactive point source is broader compared to a conventional source because of the enhanced self absorption of the radiation in the source. Moreover, enhanced Compton scattering of the radiation by a transition coming from an excited state above the first excited state, which cannot be fully discriminated, induces an enhanced background that reduces drastically the observed effect. As a result subtle hyperfine interactions cannot be unambiguously detected in microscopic samples using conventional Mössbauer spectroscopy.

In this study, we consider the advantages and disadvantages of a Synchrotron radiation Mössbauer Source (SMS); see Section 2, Nuclear Forward Scattering (NFS) of synchrotron radiation; see Section 3, and Synchrotron Radiation Perturbed Angular Correlation Spectroscopy (SRPAC); see Section 4, in order to explore the elusive and long-sought hyperfine interactions in the high pressure – room temperature phase of Fe.

2 Synchrotron radiation Mössbauer source

To eliminate all effects relevant to conventional Mössbauer spectroscopy utilizing a radioactive source we used a synchrotron radiation source. Synchrotron Mössbauer spectroscopy was carried out on a $1\ \mu\text{m}$ thick iron foil 95% enriched in ^{57}Fe . The high pressure conditions were generated using a cylindrical-type BX-90 diamond anvil cell [1] with $250\ \mu\text{m}$ culet diamonds. A Re gasket (with an initial hole diameter of $100\ \mu\text{m}$ and a thickness of about $30\ \mu\text{m}$) was used as a pressure chamber. Ar was used as a pressure transmitting medium. The sample was loaded into the pressure chamber together with several ruby chips at ambient pressure and the fluorescence of ruby chips was used as a pressure marker. The pressure chamber was compressed to $59.2(5)\ \text{GPa}$. The synchrotron Mössbauer source spectrum was recorded at the Nuclear Resonance beamline ID18 [2] of the European Synchrotron Radiation Facility using the (1 1 1) Bragg reflection of a $^{57}\text{FeBO}_3$ single crystal mounted on a Wissel velocity transducer driven with a sinusoidal waveform [3]. The X-ray beam was focused to $15\ \mu\text{m}$ vertically and $12\ \mu\text{m}$ horizontally using Kirkpatrick-Baez mirrors. The linewidth of the synchrotron Mössbauer source and the absolute position of the central shift was controlled before and after the measurement using a $\text{K}_2\text{Mg}^{57}\text{Fe}(\text{CN})_6$ reference single line absorber. The velocity scale was calibrated using a $25\ \mu\text{m}$ thick natural $\alpha\text{-Fe}$ foil. The linewidth of the source was $0.145(14)\ \text{mm/s}$ FWHM or $1.49\ \Gamma_0$. Notably, the linewidth of the source might be further reduced by adjusting the temperature of the $^{57}\text{FeBO}_3$ crystal but in this case the intensity might be highly reduced and will make the measurement not practically feasible anymore.

The spectrum shown in Fig. 1 was measured for about 8 hours. A splitting in the resonance line is not observed. The spectrum was fitted with a doublet using a full transmission integral with a normalized Lorentzian-squared source lineshape using the MossA software package [4]. The quadrupole splitting is fixed to $0.058\ \text{mm/s}$ (corresponding to about $2.7\ \text{neV}$); see Table 1. Such a fit results in a central shift of $-0.38(2)\ \text{mm/s}$ and a linewidth of $0.40(7)\ \text{mm/s}$. Distinguishing such a small broadening coming from a quadrupole splitting from other contributions such as a tiny isomer shift distribution due to a negligible small pressure gradient is nearly impossible. As a result, we can reasonably assume that the existence of a hyperfine interaction which might result in a tiny energy splitting in

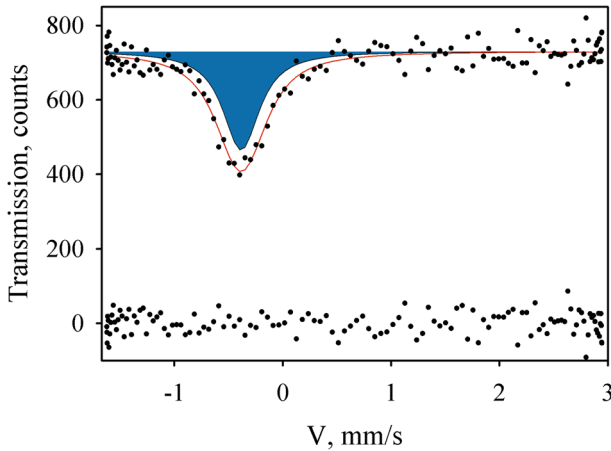


Fig. 1 Synchrotron Mössbauer source spectrum measured on hexaferrum loaded in Ar at 59.2(5) GPa. The blue shaded region shows the theoretical fit to a doublet with a quadrupole splitting fixed to 0.058 mm/s (corresponding to 2.6 neV). The solid red curve is a convolution of the absorption line of the sample with the emission line of the source and gives a hint about the additional broadening due to sample thickness. The fit residuals are indicated as points at the bottom of the figure

Table 1 The parameters obtained from fitting the model described in (1) to the experimental data shown in Fig. 5: τ is the characteristic decay time, A_{22} is the anisotropy factor, ω is the characteristic frequency for the hyperfine interactions, and δE is the extracted hyperfine energy splitting

Pressure	Structure	Hyperf. interact.	τ (ns)	A_{22}	ω (rad/ns)	δE (neV)
Ambient	bcc	magnetic	144.6(12)	0.096(7)	0.1633(4)	107.4(3)
13(1) GPa	bcc	magnetic	143.2(15)	0.087(12)	0.1608(8)	105.8(5)
25(1) GPa	hcp	electric	149.2(9)	0.103(16)	0.0039(7)	2.6(5)
25(1) GPa	hcp	magnetic	149.2(9)	0.136(25)	0.0024(4)	1.6(3)

the nuclear energy levels of ^{57}Fe cannot be unambiguously observed by Mössbauer spectroscopy (neither using a conventional radioactive source nor a synchrotron source) in the energy domain.

3 Nuclear forward scattering of synchrotron radiation

Nuclear Forward Scattering (NFS) [5, 6] of synchrotron radiation is an elastic – coherent process and the analog of Mössbauer spectroscopy in time domain. NFS is currently a routine characterization method in order to study hyperfine interactions in samples under extreme conditions or in surfaces, i.e., monolayers, multilayers.

Figure 2 shows a simulation of the nuclear forward scattering intensity in hexaferrum (with a natural abundance in ^{57}Fe) of extremely different thicknesses without or with the presence of a hyperfine interaction of electric origin.

In case of a 50 nm thick sample with the presence of a hyperfine interaction of electric origin which leads to energy splitting of $0.67 \Gamma_0$ in the nuclear levels a first minimum around

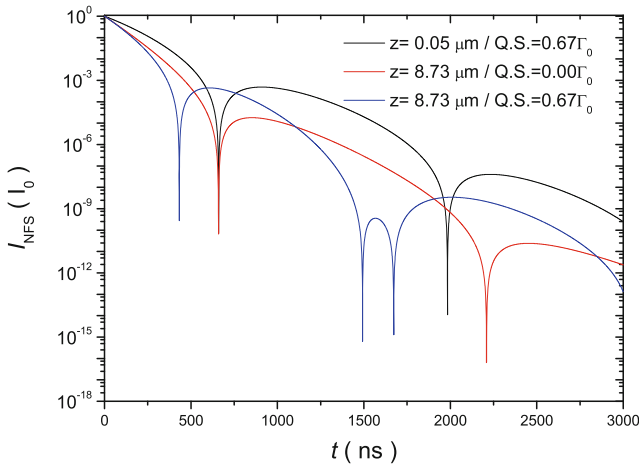


Fig. 2 Simulation of NFS spectra of hexaferrum with a natural abundance in ^{57}Fe with thickness, z , of 0.05 and 8.73 μm and a magnitude of nuclear quadrupole splitting (Q.S.) $0.67\Gamma_0$ and $0.00\Gamma_0$

600 ns and a second minimum around 2 μs is observed in the nuclear forward scattering spectrum.

In case of a 8.73 μm thick sample without the presence of any hyperfine interaction the first minimum in the NFS spectrum appears at the same time with the previous case but the second minimum appears around 2.25 μs .

In case of a 8.73 μm thick sample with the presence of a hyperfine interaction of electric origin which leads to an energy splitting in the nuclear levels of $0.67\Gamma_0$ a first minimum around 450 ns appears and the shape of the curve after 1.5 μs is totally different than in the previous two cases.

It is well known that the thicker the sample the more the first minimum shifts to earlier time. However, the experimentally observed shift may be the result of the presence of a hyperfine interaction alone, of thickness effects, or a combination of both cases.

In summary, there are two major drawbacks of NFS in detecting a very small energy splitting in the nuclear levels. NFS is a coherent process where scattering occurs only in the forward direction. The effective nuclear thickness of the sample has a primary contribution in the observed beating of the NFS spectra. As a result, it is not trivial to distinguish hyperfine interactions from variations of geometrical sample thickness which result in the so-called hybrid beats, i.e., a combination of both contributions. In addition, subtle hyperfine interactions usually lead to a very low beating frequency in the time spectrum, see e.g., Fig. 2. In such a case the second or third quantum beat, which is the critical quantum beat in order to distinguish the nature of the hyperfine interaction, may appear at a very late time where the recorded intensity coming from the nuclear decay may be comparable with the recorded background. Thus, NFS does not seem to be a viable method for hyperfine interactions characterization of samples with a subtle energy splitting in the nuclear levels.

4 Synchrotron radiation perturbed angular correlation spectroscopy

Synchrotron Radiation Perturbed Angular Correlation (SRPAC) spectroscopy is an inelastic – incoherent process [7]. SRPAC combines all features of synchrotron radiation, i.e., high

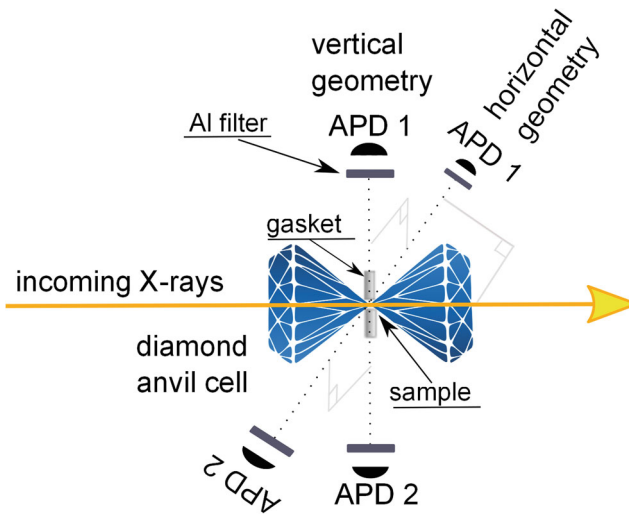


Fig. 3 The SRPAC experimental setup used in this study includes a ^{57}Fe sample located in a diamond anvil cell and a set of detectors (APD1 and APD2). The relative position of the detectors for the vertical and horizontal geometry is shown

brilliance, small beamsize, with all features of Time Domain Perturbed Angular Correlation (TDPAC) [8, 9] spectroscopy, i.e., the sample thickness does not contribute to the TDPAC signal, the radioactive source resonance line broadening is absent. The main strength of this characterization technique is, however, that between all contributions in the measured incoherent signal only SRPAC in the presence of a hyperfine interaction is anisotropic. The electromagnetic radiation - X-rays - absorbed by the sample come from a well defined direction and has a well defined polarization. Thus, the angular distribution of the emitted radiation depends on the orientation of the nuclear spin at the time the radiation is emitted.

The SRPAC measurements in this study were carried out at the Nuclear Resonance beamline ID18 [2] at the European Synchrotron Radiation Facility. We used a Fe sample 96% enriched to ^{57}Fe . The crystallographic purity of the sample was checked at ambient conditions using X-ray diffraction at P02.2/PETRA III beamline. The sample comprised a single bcc-Fe phase. The sample was loaded together with several ruby chips in a $30\ \mu\text{m}$ pre-indented beryllium gasket between two diamond anvils of $300\ \mu\text{m}$ culet diameter. In order to achieve reasonable hydrostatic conditions up to 25 GPa paraffin oil was used as a pressure transmitting medium. The pressure in the sample space was measured before and after the actual SRPAC measurement using the ruby fluorescence method. The mean pressure values and the error bars are given in Table 1. The X-ray beam was focused using two multilayer mirrors in Kirkpatrick-Baez configuration to $7\ \mu\text{m}$ vertically and $15\ \mu\text{m}$ horizontally.

In this study, we utilized a monochromator with an energy bandpass of 15 meV (full-width at half maximum) at the nuclear resonance energy of ^{57}Fe at 14.412 keV and the data was measured at +30 meV relative to the nuclear resonance energy (in the phonon creation side). Moreover, background measurements at -250 meV relative to the nuclear resonance energy (in the phonon annihilation side) were carried out in turn with the actual SRPAC measurements and although negligible it was taken into account in the data treatment.

The temporal evolution of the SRPAC signal was detected between 20 and 700 ns after the arrival of the X-ray pulses, which in 4 bunch mode arrive every 704 ns. Avalanche Photo

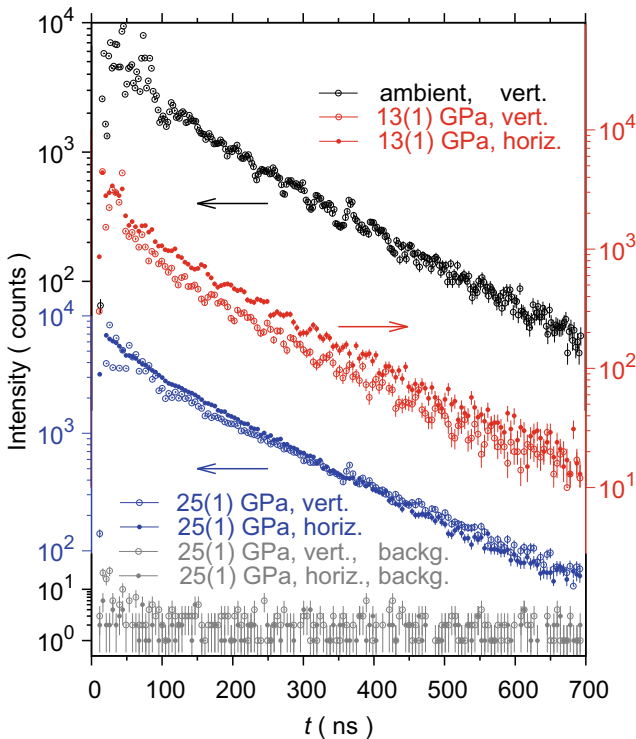


Fig. 4 The temporal evolution of the intensity registered at room temperature and ambient pressure in vertical geometry, at 13(1) GPa, and at 25(1) GPa in both vertical and horizontal geometries and the corresponding background measurement at 25(1) GPa. Characteristic error bars are given

Diode (APD) detectors with 200 μm thick active area of 10 mm x 10 mm were used. The APDs were placed at a distance of 6 mm from the sample in opposite sides of the pressure cell and were covered with a 320 μm thick high purity aluminium foil in order to suppress the delayed 6.4 keV Fe $K\alpha$ fluorescence arising from nuclear internal conversion.

In order to explore the spatial anisotropy of the SRPAC data, the SRPAC measurements were carried out in vertical and horizontal scattering geometry, see Fig. 3.

The change between the two geometries was reproducibly done through rotation of the high pressure cell holder together with the detectors, which were attached to it, relative to the X-ray beam. Special attention was paid to probe the sample (within the beamsizes) at the same spot.

The raw background measurement at 25(1) GPa together with the raw spectra measured at ambient pressure¹ in the vertical geometry, at 13(1) GPa and at 25(1) GPa in both vertical and horizontal geometries are shown in Fig. 4. The background subtracted data were divided by an exponential decay with a characteristic decay time, see Table 1, and are shown in Fig. 5.

¹The SRPAC measurements carried out in the so-called ambient conditions were done after releasing the pressure in the diamond anvil cell. The sample may experience a residual pressure in these conditions.

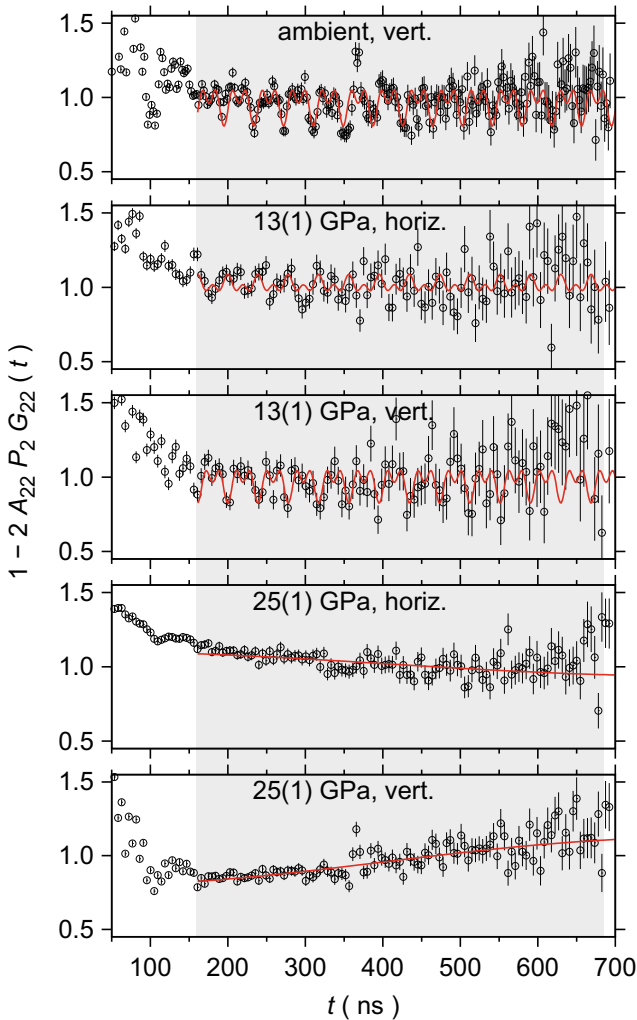


Fig. 5 The temporal evolution of the anisotropy factor, $1-2A_{22}P_2G_{22}(t)$, registered at ambient pressure and room temperature using a 15 meV energy resolution in vertical geometry, at 13(1) GPa, and at 25(1) GPa in both vertical and horizontal geometries. The red solid line is the fit performed in the highlighted area according to the model described in (1)

Figure 5 shows the temporal evolution of the anisotropy factor, i.e., $1-2A_{22}P_2G_{22}(t)$; see (1), obtained from the data shown in Fig. 4. Characteristic high frequency modulations between 160 and 500 ns are observed in the spectra at ambient pressure, and at 13(1) GPa. Note that the modulations at 13(1) GPa data are inverted for the vertical and horizontal geometry due to the anisotropy of the SRPAC signal. In the spectra measured at 25(1) GPa high frequency modulations are not observed. Low frequency modulations inverted in the horizontal and vertical geometry are seen instead. This is the evidence for the existence of a finite hyperfine splitting. An up-turn in the temporal evolution of the anisotropy at time earlier than 150 ns for both vertical and horizontal geometry is observed. This effect is pronounced because a monochromator with a broad energy bandpass was used, thus, there

is a sizeable probability for nuclear forward scattering events to occur because the tails of the energy bandpass overlap with the nuclear resonance energy. Thus, this effect can be safely attributed to Rayleigh scattering following a nuclear forward scattering event [10].

The theoretical model for the temporal evolution of the SRPAC signal in the case of randomly oriented hyperfine fields is summarized in (1) [10, 11].

$$I(t) = I_0 \exp(-t/\tau)(1 - 2A_{22}P_2G_{22}(t)) \quad (1)$$

where I_0 is an intensity scaling factor, τ is a characteristic decay time, A_{22} is a factor which is defined by the nuclear transition and details of the experimental setup such as the sample to detector distance, e.g., when the detector is far away from the sample the observed countrate will be close to zero and no SRPAC signal will be detected. In the opposite case, when the detector is very close to the sample the countrate will be maximal but the anisotropy coefficient A_{22} will be close to zero due to spatial averaging, P_2 is a geometry factor, i.e., $P_2 = 1$ for the vertical geometry and $P_2 = -1/2$ for the horizontal geometry, and $G_{22}(t)$ is the perturbation factor which describes the temporal modulation of the signal $G_{22}^{magn}(t) = 1/5(1 + 2\cos\omega t + 2\cos 2\omega t)$ due to magnetic hyperfine interactions and for electric hyperfine interactions $G_{22}^{elect}(t) = 1/5(1 + 4\cos\omega t)$, where ω is the characteristic angular frequency of the modulation.

A fit of the model summarized in (1) to the experimental data shown in Fig. 5 is carried out. The data in the vertical and horizontal geometry was fitted with a common set of parameters. The values extracted for A_{22} , ω , and the energy splitting δE are shown in Table 1. An increase of A_{22} when magnetic hyperfine interactions are included in the fit at 25(1) GPa is observed $A_{22} = 0.136(25)$ compared to the average $A_{22} = 0.095(3)$ obtained from all other cases shown in Table 1.

The decay time τ is larger than the natural lifetime, i.e., 141.11 ns for the first excited state of ^{57}Fe , by 2% in α -Fe and by 6% in ε -Fe. Such an increase is expected from radiation trapping [12]. The relative increase in τ between α -Fe and ε -Fe is due to the increased nuclear absorption caused by the collapse of the hyperfine magnetic field. The anisotropy constant A_{22} is within the error bar the same for all but one fit.

The modulations observed at 25(1) GPa in ε -Fe with a characteristic frequency $\omega = 0.0039(7)$ rad/ns do not include an entire period and can be fitted using both electric and magnetic hyperfine interactions, see Table 1.

A hint about the nature of the hyperfine interaction in ε -Fe might be obtained from the present data. The A_{22} parameter is independent of the nature of the hyperfine interaction. However, the fit of the SRPAC spectra at 25 GPa with a model which includes magnetic hyperfine interactions requires an increase of the A_{22} by $\sim 30\%$, which is not the case when the SRPAC spectra at 25 GPa are fitted with a model that includes an electric hyperfine interaction. The increase of A_{22} is not physically meaningful and indicates that the model of magnetic interactions is much less probable. Thus, the results evidence that the observed hyperfine splitting is caused mainly by a quadrupole interaction, though the presence of a small magnetic field superimposed to the electric field gradient cannot be fully excluded.

In summary, SRPAC is a viable method for hyperfine interactions characterization in samples with subtle hyperfine interactions which result in a tiny splitting in the nuclear levels. A potential limitation in SRPAC data treatment is the observed Rayleigh scattering following a nuclear forward scattering event. In order to circumvent this problem a monochromator with a narrow bandpass must be used and the SRPAC measurements may preferably be carried out at an energy as far away from the elastic line as possible.

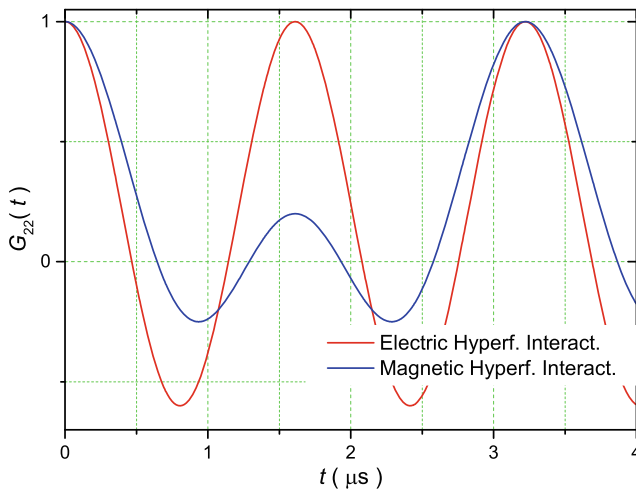


Fig. 6 Simulation of the temporal evolution of the perturbation factor $G_{22}(t)$ for the electric and magnetic hyperfine interactions. The characteristic frequencies, ω are taken from Table 1 for the case of 25(1) GPa

5 Outlook

An unambiguous distinction between the nature of hyperfine interactions would be possible using a larger time window. A simulation of the temporal evolution of the perturbation factor $G_{22}(t)$; see (1) involved in the SRPAC data treatment for an extended time window up to 4 μs is depicted in Fig. 6 for both electric and magnetic hyperfine interactions. It is evident that the temporal evolution of the modulations are clearly different for electric and magnetic hyperfine interactions.

In order to unambiguously attribute the observed energy splitting in the nuclear levels of ^{57}Fe to an electric or magnetic origin SRPAC measurements up to 1-1.5 μs should be carried out. However, such measurements today are not feasible. Increasing the energy bandwidth of the incoming X-rays does not really help because the tails of the instrumental function strongly overlap with the nuclear resonance energy and non trivial multiple scattering phenomena take place; see Section 4. Thus, in order to achieve a reasonable signal to noise ratio in a more extended time window, 2-3 orders of magnitude more photon flux is currently missing. Notably, this problem is not going to be solved in the so-called 4th generation synchrotron radiation storage rings which are currently under development.

A potential solution is the use of an X-ray Free Electron Laser Oscillator (XFEL) seeded at the nuclear resonance energy of ^{57}Fe [13]. The radiation load on the detector in SRPAC measurements is not expected to be too serious because in SRPAC the direct beam is not intercepted. Moreover, the radiation load on the detector could be alleviated by e.g., substituting a single detector with many small detectors covering a small solid angle each.

Acknowledgements The European Synchrotron Radiation Facility is acknowledged for beamtime provision at the Nuclear Resonance beamline ID18. We thank Mr. J.-P. Celse for technical assistance during the experiment at ID18 and Prof. Leonid Dubrovinsky for providing the diamond anvil cells.

Compliance with Ethical Standards

Conflict of interests The authors declare that they have no conflict of interest.

References

1. Kantor, I., Prakapenka, V., Kantor, A., Dera, P., Kurnosov, A., Sinogeikin, S., Dubrovinskaia, N., Dubrovinsky, L.: BX90: A new diamond anvil cell design for X-ray diffraction and optical measurements. *Rev. Sci. Instrum.* **83**, 125102 (2012)
2. Ruffer, R., Chumakov, A.I.: Nuclear Resonance Beamline at ESRF. *Hyperfine Interact.* **97–98**, 589 (1996)
3. Potapkin, V., Chumakov, A.I., Smirnov, G.V., Celse, J.P., Ruffer, R., McCammon, C., Dubrovinsky, L.: The ^{57}Fe synchrotron Mössbauer source at the ESRF. *J. Synchrotron Radiat.* **19**, 559 (2012)
4. Prescher, C., McCammon, C., Dubrovinsky, L.: MossA: a program for analyzing energy-domain Mössbauer spectra from conventional and synchrotron sources. *J. Appl. Crystallogr.* **45**, 329 (2012)
5. Hastings, J.B., Siddons, D.P., van Bürck, U., Hollatz, R., Bergmann, U.: Mössbauer spectroscopy using synchrotron radiation. *Phys. Rev. Lett.* **66**, 770 (1991)
6. van Bürck, U., Siddons, D.P., Hastings, J.B., Bergmann, U., Hollatz, R.: Nuclear forward scattering of synchrotron radiation. *Phys. Rev. B* **46**, 6207 (1992)
7. Baron, A.Q.R., Chumakov, A.I., Ruffer, R., Grünsteudel, H., Grünsteudel, H.F., Leupold, O.: Single-nucleus quantum beats excited by synchrotron radiation. *Europhys. Lett.* **34**, 331 (1996)
8. Soares, J.C., Krien, K., Bibiloni, A.G., Freitag, K., Vianden, R.: Determination of the quadrupole splitting of the first excited state of ^{119}Sn in β -tin by the $e^- - \gamma$ TDPAC technique. *Phys. Lett. A* **45**, 465 (1973)
9. Hohenemser, C., Erno, R., Benski, H.C., Lehr, J.: Time-differential perturbed angular-correlation experiment for ^{57}Fe in a Ni host, and a comparison with the Mössbauer effect. *Phys. Rev.* **184**, 298 (1969)
10. Sergueev, I., van Bürck, U., Chumakov, A.I., Asthalter, T., Smirnov, G.V., Franz, H., Ruffer, R., Petry, W.: Synchrotron-radiation-based perturbed angular correlations used in the investigation of rotational dynamics in soft matter. *Phys. Rev. B* **73**, 024203 (2006)
11. Sergueev, I., Leupold, O., Wille, H.-C., Roth, T., Chumakov, A.I., Ruffer, R.: Hyperfine interactions in ^{61}Ni with synchrotron-radiation-based perturbed angular correlations. *Phys. Rev. B* **78**, 214436 (2008)
12. Chumakov, A.I., Metge, J., Baron, A.Q.R., Ruffer, R., Shvyd'ko, Yu.V., Grünsteudel, H., Grünsteudel, H.F.: Radiation trapping in nuclear resonant scattering of X-rays. *Phys. Rev. B* **56**, R8455 (1997)
13. Adams, B., Aeppli, G., Allison, T., Baron, A.Q.R., Bucksbaum, P., Chumakov, A.I., Corder, C., Cramer, S.P., DeBeer, S., Ding, Y., Evers, J., Frisch, J., Fuchs, M., Grübel, G., Hastings, J.B., Heyl, C.M., Holberg, L., Huang, Z., Ishikawa, T., Kaldun, A., Kim, K.-J., Kolodziej, T., Krzywinski, J., Li, Z., Liao, W.-T., Lindberg, R., Madsen, A., Maxwell, T., Monaco, G., Nelson, K., Palfy, A., Porat, G., Qin, W., Raubenheimer, T., Reis, D.A., Röhlberger, R., Santra, R., Schoenlein, R., Schünemann, V., Shpyrko, O., Shvyd'ko, Yu., Shwartz, S., Singer, A., Sinha, S.K., Sutton, M., Wille, K., Tamasaku, H.-C., Yabashi, M., Ye, J., Zhu, D.: Scientific opportunities with an X-ray free-electron laser oscillator. [arXiv:1903.09317](https://arxiv.org/abs/1903.09317) (2019)

Publisher's note Springer Nature remains neutral with regard to jurisdictional claims in published maps and institutional affiliations.